Towards a unified low frequency Stability criterion for 15 kV / 16.7 Hz and 25 kV / 50 Hz railway power system

Y. Hachicha[1,2], D. Cypers[1], S. Belin[1], M. Meli[1], P. Ladoux[2], N. Roux[2]

[1] Alstom, Tarbes, France
[2] Université de Toulouse, CNRS, INPT, UPS, Toulouse, France

Corresponding author: David CYPERS, david.cypers@alstomgroup.com

Abstract

Low frequency voltage instabilities of the AC railway networks are due to the interactions between modern traction vehicles and infrastructure. These instabilities can lead to a large amplitude modulation of the catenary voltage that can cause train power supply shut down or damage on traction equipment. This paper presents a straightforward method for determining the stability limit of a railway power system which is applicable to both 25 kV / 50 Hz and 15 kV / 16.7 Hz networks. This approach is the first step to define a unique stability criterion for both networks. The method is based on the stability limit curve of a traction chain plotted in the complex impedance plane (R, X). The validation of this method is performed through the use of a HIL (Hardware In the Loop) simulator.

1 Introduction

Low-frequency instabilities that have appeared on the AC railway networks are due to the massive introduction of traction vehicles equipped with Four-Quadrant (4-Q) rectifiers and the increase in railway traffic. These instabilities appear as an amplitude modulation of the catenary voltage and current at very low frequency and can lead to train power supply shut down. The first case of low frequency instability that occurred in northeastern France near the town of Thionville in 2008 is shown in Fig. 1 [1].

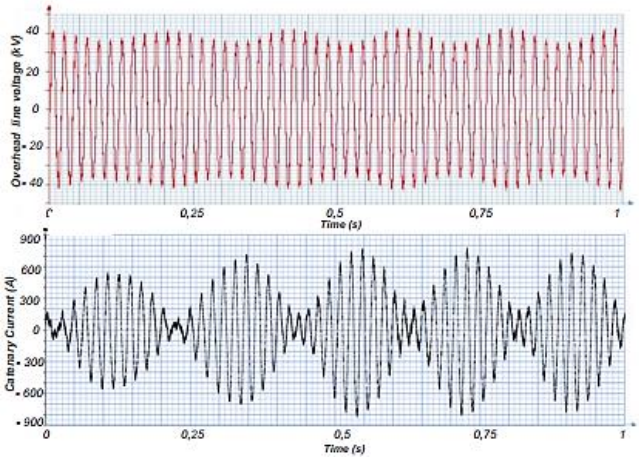

Fig. 1: Modulation of catenary voltage and current measured at the substation in Thionville – France (25 kV / 50 Hz power supply).

Several studies were carried out in order to determine the origins of the phenomenon [2], [3], [4].

The power system composed of a traction chain and a power supply network can be represented as a closed-loop system (see Fig. 2). Y is the admittance of a traction chain and Z is the power supply network impedance. U_0 and U_p are the no-load voltage and the pantograph voltage, respectively.

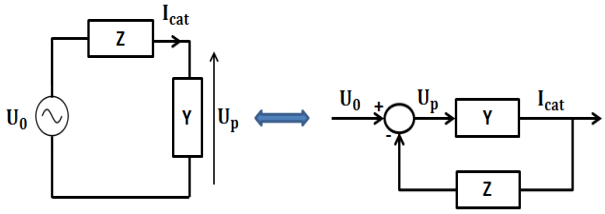

Fig. 2: Closed-loop power system.

This power system is simulated with the Alstom HIL simulator (SITRA^{TM}). The traction control device used on the train (AGATE: Advanced Generic Alstom Transport Electronics) is also used to control the traction chain simulated in SITRA.

As explained in [5], the power supply and the traction unit have to be considered as a MIMO (Multiple-Input and Multiple-Output) system in the d-q frame. The network impedance matrix Z_{DQ} and the traction chain admittance matrix Y_{DQ} are given below:

- $Z_{DQ}(j \cdot \omega) = \begin{pmatrix} Z_{dd}(j \cdot \omega) & Z_{dq}(j \cdot \omega) \\ Z_{qd}(j \cdot \omega) & Z_{qq}(j \cdot \omega) \end{pmatrix} = \begin{pmatrix} R + j \cdot L \cdot \omega & -L \cdot \omega_n \\ L \cdot \omega_n & R + j \cdot L \cdot \omega \end{pmatrix}$ (1)

: R and L are the resistance and inductance of the network and ω_n is the nominal angular frequency of the network. ω is the perturbation angular frequency ($\omega = 2\pi \cdot f$ (2)).

- $Y_{DQ}(j \cdot \omega) = \begin{pmatrix} Y_{dd}(j \cdot \omega) & Y_{dq}(j \cdot \omega) \\ Y_{qd}(j \cdot \omega) & Y_{qq}(j \cdot \omega) \end{pmatrix}$ (3)

In our case, the traction chain is simulated in SITRA and the admittance matrix components are determined according to the method proposed in [3].

The open-loop transfer function of the traction system can be expressed as:

$H_{BO}(j \cdot \omega) = Z_{DQ}(j \cdot \omega).Y_{DQ}(j \cdot \omega) = P^{-1}.D.P$ (4)

- $D = \begin{pmatrix} \lambda_1(j \cdot \omega) & 0 \\ 0 & \lambda_2(j \cdot \omega) \end{pmatrix}$ (5): Eigenvalues matrix of the $H_{BO}(j \cdot \omega)$.

- P: Eigenvectors matrix of the $H_{BO}(j \cdot \omega)$.

It is only necessary to study the stability of each eigenvalue in order to study the stability of the traction system since D matrix allows to have two decoupled SISO (Single-Input and Single-Output) systems (λ_1 and λ_2). The stability criterion of the SISO system used is based on the Rever's criterion applied in the Bode plot: the system is at its stability limit if at the frequency f_c for which $Arg(H_{BO}(j \cdot 2\pi \cdot f_c)) = -180°$ (6), the module in dB of the open-loop transfer function is equal to 0 dB.

[5] presents the stability study of a power system for three given impedance values using the theorem defined above. The same resistance (R) value, arbitrarily chosen, was used for the three tests and only the inductance (L) value was changed in order to have the three cases of stability (stable, limit of stability and unstable). The coherence between frequency analysis and temporal analysis was also verified.

[6] presents the stability study of a traction chain (simulated with PC simulation software) supplied by a 25 kV / 50 Hz network for different values of (R, L). The stability limit curve of this traction chain is composed of all the values (R, L) allowing to verify the criterion defined above.

In this paper, the stability study is carried out on several projects (traction chain simulated in SITRA), checking each time the coherence between the time domain and the frequency domain.

2 Determination of the traction system's stability for different traction chains

As explained in [6], the stability limit of a power system is obtained by using three iterative loops. The first loop is used to modify the value of the supply network resistance (R); the second loop modifies its inductance (L) and the third loop allows to browse all the frequencies for which the admittance of the traction chain has been calculated (f). The stability criterion (Rever's criterion applied in the Bode plot) has been adapted by adding phase and gain margins because the frequency discretization of the admittance matrix elements does not allow an exact extraction of the corresponding values of R and L which bring the system to its limit of stability:

- $-180° < Arg(\lambda) < -178°$
- $-0.1\ _{dB} < |\lambda|\ _{dB} < 0\ _{dB}$

2.1 Traction chain supplied by a 25 kV / 50 Hz network (25 kV Project)

The traction chain considered in this section is composed of a step-down transformer with two secondary windings, two (4-Q) rectifiers and a current source connected to the common DC bus (see Fig .3). This source represents the current absorbed by the traction inverters and the auxiliary inverter. This traction chain is supplied by a 25 kV / 50 Hz network.

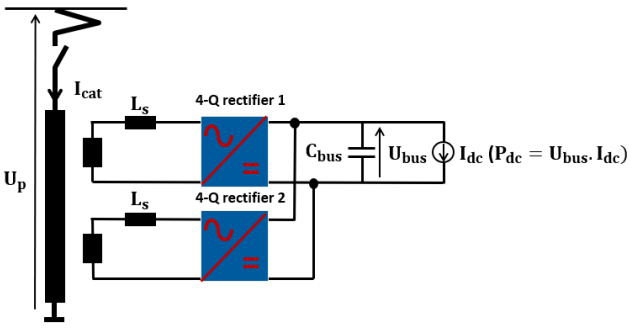

Fig. 3: Traction chain simulated in SITRA.

This project (supply network and traction chain) will be called "25 kV Project" in the rest of this paper.

The stability limit of this system when the power absorbed on the DC bus (P_{dc}) is 100 kW was

determined and plotted in the network impedance plane (R, X = L.ω_n (7)) (see Fig. 4).

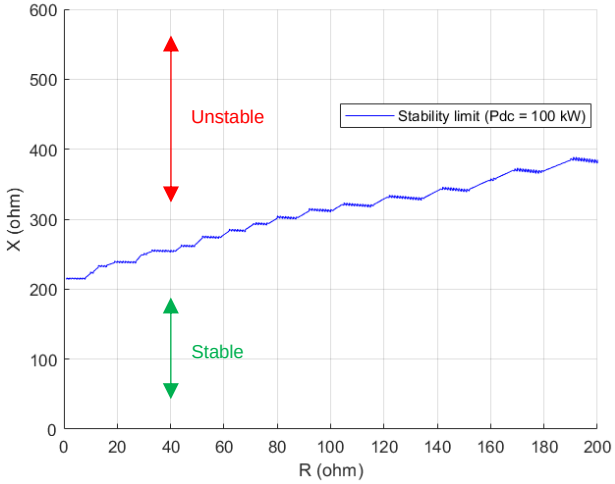

Fig. 4: Stability limit curve of a traction chain supplied by a 25 kV / 50 Hz network (P_{dc} = 100 kW).

Three network impedance values were tested in order to validate this stability study: the first impedance (R, X) chosen is below the stability limit curve (stable case); the second impedance (R, X) chosen is on the stability limit curve and the last point (R, X) is above the stability limit curve (unstable case).

For time domain simulations, the voltage source amplitude has been adapted according to the network impedance used in order to always have a pantograph voltage equal to 25 kV. This is due to the fact that the admittance of the traction chain was determined by considering that the pantograph is connected to an ideal voltage source of 25 kV.

$$U_0^2 = (R \cdot I_{cat} + U_p)^2 + (X \cdot I_{cat})^2 \quad (8)$$

- **Case 1: Stable system**
  R = 100 Ω; L = 0.79 H:

Frequency analysis based on admittance matrix measurement and Rever's criterion applied to the system's eigenvalues:

The Bode diagram of the system's eigenvalues is shown in Fig. 5. This system is stable since the gain of the second eigenvalue is negative when its phase is around (-180°) and the phase of the first eigenvalue is always greater than (-180°).

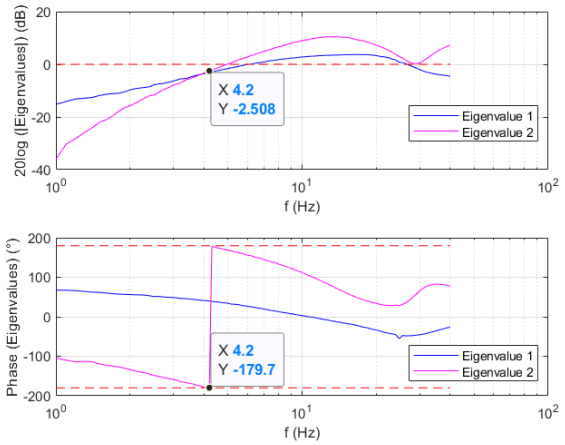

Fig. 5: Bode diagram of the system's eigenvalues (25 kV Project - Case 1).

Time domain simulation:

Figure 6 presents the waveforms of the voltage and the current at the pantograph as well as the DC link voltage of the traction chain. This time-domain simulation effectively shows that the system is stable.

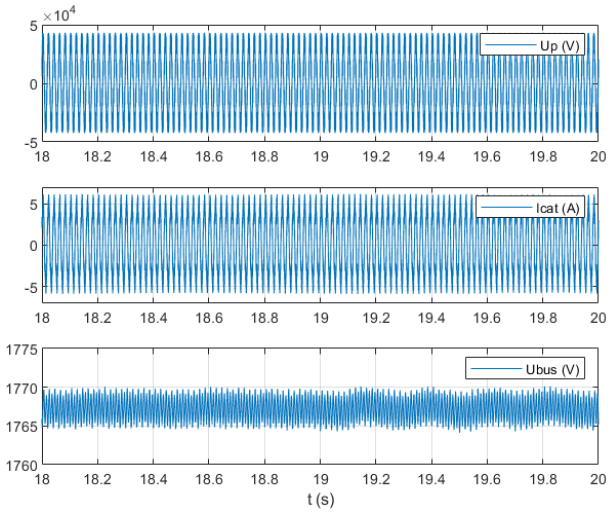

Fig. 6: 25 kV Project - Case 1. Time domain simulations: Pantograph voltage, Catenary current and DC bus voltage waveforms.

- **Case 2: System at its stability limit**
  R = 100 Ω; L = 0.95 H:

Frequency analysis based on admittance matrix measurement and Rever's criterion applied to the system's eigenvalues:

The Bode diagram of the system's eigenvalues is shown in Fig. 7. This system is at its stability limit

since the gain of eigenvalue 2 is almost zero dB when its phase is around (-180°) and the phase of the first eigenvalue is always greater than (-180°). The oscillation frequency is 4.3 Hz.

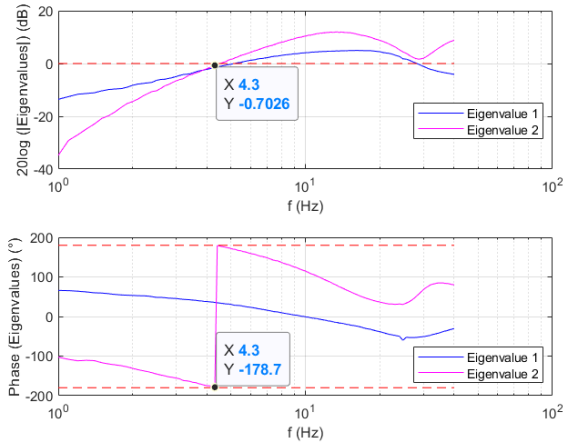

Fig. 7: Bode diagram of the system's eigenvalues (25 kV Project - Case 2).

Time domain simulation:

Figure 8 shows the waveforms of the voltage and the current at the pantograph as well as the DC link voltage of the traction chain.

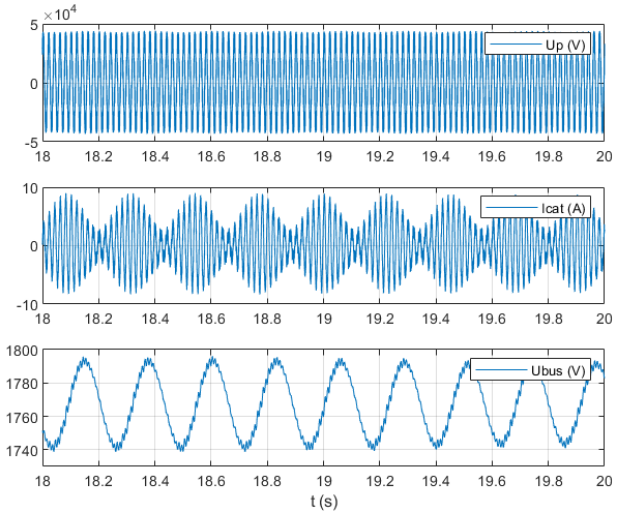

Fig. 8: 25 kV Project - Case 2. Time domain simulations: Pantograph voltage, Catenary current and DC bus voltage waveforms.

The result obtained in the frequency domain is validated in the time domain since all the waveforms present a low frequency amplitude modulation at a frequency equal to 4.35 Hz.

- **Case 3: Unstable system R = 100 Ω; L = 1.18 H:**

Frequency analysis based on admittance matrix measurement and Rever's criterion applied to the system's eigenvalues:

The Bode diagram of the system's eigenvalues is shown in Fig. 9. This system is unstable since the gain in dB of one of its eigenvalues is positive when its phase is equal to (-180°).

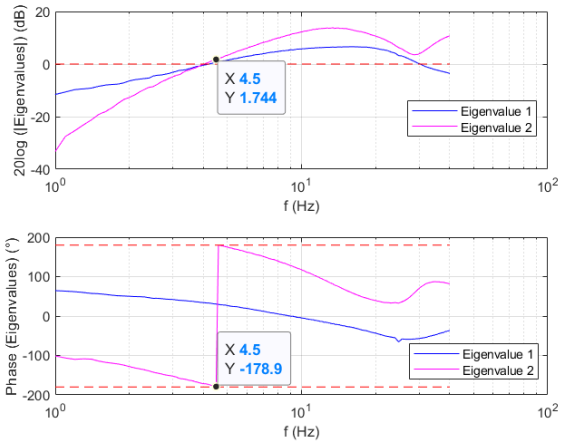

Fig. 9: Bode diagram of the system's eigenvalues (25 kV Project - Case 3).

Time domain simulation:

The waveforms of Fig. 10 clearly show that the system is unstable. A huge voltage ripple is observed on the DC bus while the catenary current shows discontinuities.

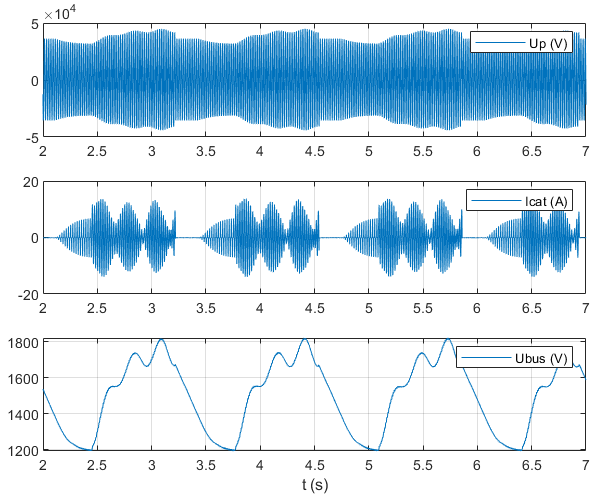

Fig. 10: 25 kV Project - Case 3. Time domain simulations: Pantograph voltage, Catenary current and DC bus voltage waveforms.

2.2 Traction chain supplied by a 15 kV / 16.7 Hz network (15 kV Project)

The project studied in this section consists of a 15 kV / 16.7 Hz network and a traction chain with a topology similar to the 25 kV Project. The installed power of this traction chain is 1 MW. This project will be called “15 kV Project” in the rest of this document.

Figure 11 shows the stability limit curve of this system when the absorbed power on the DC bus (P_{dc}) is 100 kW.

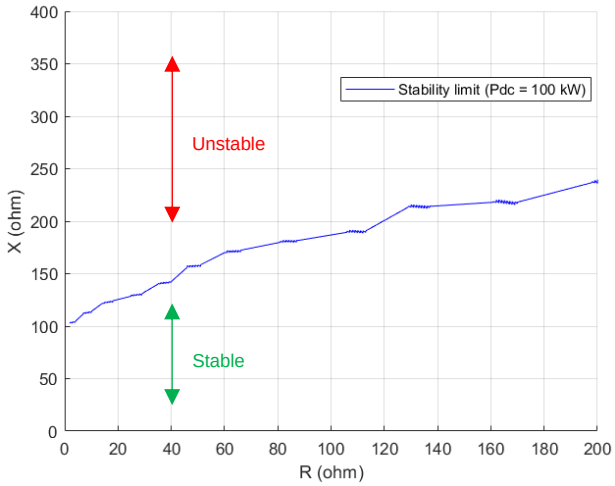

Fig. 11: Stability limit curve of a traction chain supplied by a 15 kV / 16.7 Hz network (P_{dc} = 100 kW).

Three network impedance values were tested in order to validate this stability study (stable, stability limit and unstable). For time domain simulations, the voltage source amplitude has been adapted according to the network impedance used in order to always have a pantograph voltage equal to 15 kV.

- **Case 1: Stable system R = 110 Ω; L = 1.45 H:**

Frequency analysis based on admittance matrix measurement and Rever’s criterion applied to the system’s eigenvalues:

Figure 12 shows the Bode diagram of the system’s eigenvalues. This system is stable since the gain of the first eigenvalue is negative when its phase is around (-180°) and the phase of the second eigenvalue is always greater than (-180°).

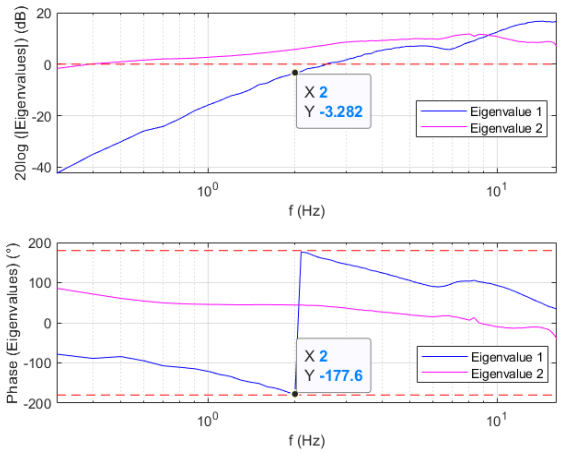

Fig. 12: Bode diagram of the system's eigenvalues (15 kV Project - *C*ase 1).

Time domain simulation:

The waveforms of the voltage and the current at the pantograph as well as the DC link voltage of the traction chain are presented in Fig. 13. This time-domain simulation effectively shows that the system is stable.

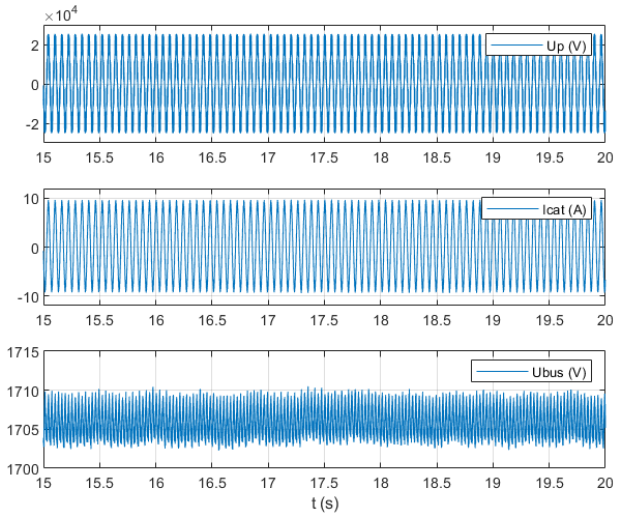

Fig. 13: 15 kV Project - Case 1. Time domain simulations: Pantograph voltage, Catenary current and DC bus voltage waveforms.

- **Case 2: System at its stability limit R = 110 Ω; L = 1.79 H:**

Frequency analysis based on admittance matrix measurement and Rever’s criterion applied to the system’s eigenvalues:

Figure 14 shows the Bode diagram of the system’s eigenvalues. This system is at its stability limit

since the gain of eigenvalue 1 is almost zero dB when its phase is around (-180°) and the phase of the second eigenvalue is always greater than (-180°). The oscillation frequency is 2.2 Hz.

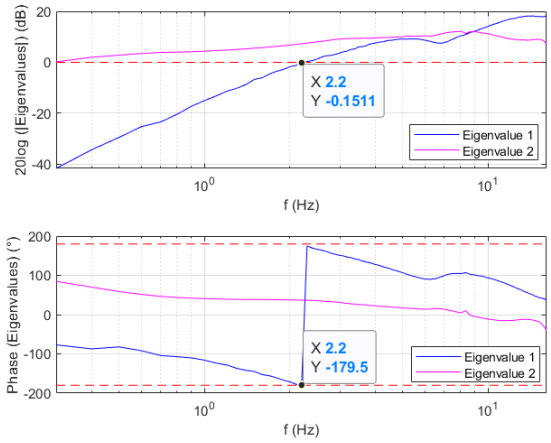

Fig. 14: Bode diagram of the system's eigenvalues (15 kV Project - Case 2).

Time domain simulation:

The waveforms of the voltage and the current at the pantograph as well as the DC link voltage of the traction chain are shown in Fig. 15.

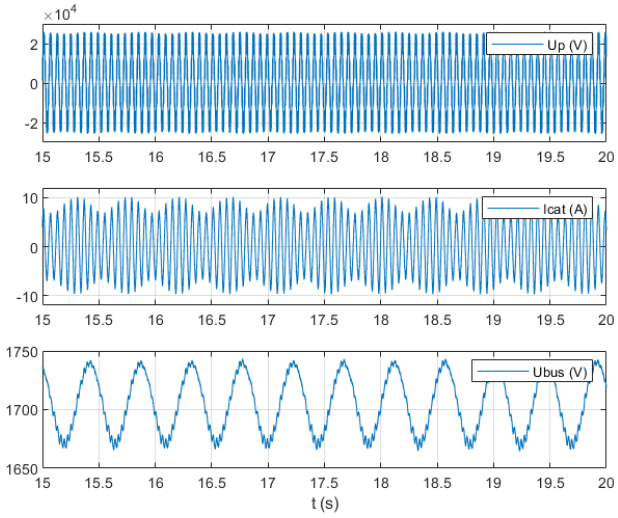

Fig. 15: 15 kV Project - Case 2. Time domain simulations: Pantograph voltage, Catenary current and DC bus voltage waveforms.

- **<u>Case 3: Unstable system R = 110 Ω; L = 2.17 H:</u>**

Frequency analysis based on admittance matrix measurement and Rever's criterion applied to the system's eigenvalues:

Figure 16 shows the Bode diagram of the system's eigenvalues. This system is unstable since the gain in dB of one of its eigenvalues is positive when its phase is equal to (-180°).

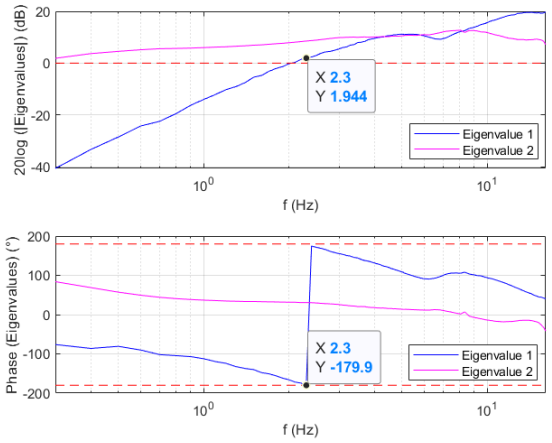

Fig. 16: Bode diagram of the system's eigenvalues (15 kV Project - Case 3).

Time domain simulation:

The waveforms of the voltage and the current at the pantograph as well as the DC link voltage of the traction chain are shown in Fig. 17. The system is unstable because all the curves diverge.

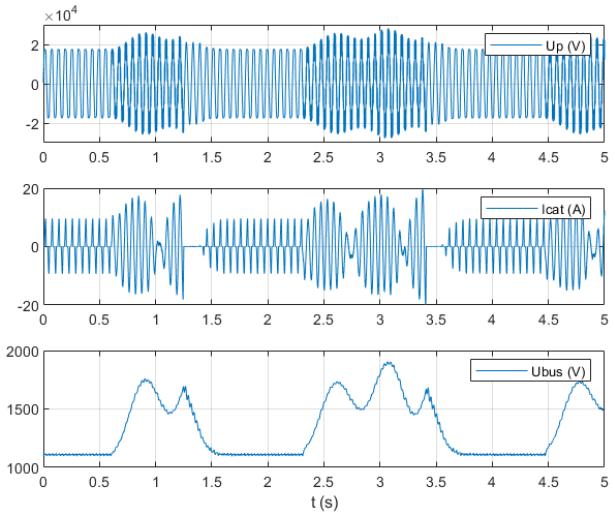

Fig. 17: 15 kV Project - Case 3. Time domain simulations: Pantograph voltage, Catenary current and DC bus voltage waveforms.

3 Evolution of the stability limit as a function of the supply network (25 kV Project / 15 kV Project)

Fig. 18 shows the traction chain stability limits of the 25 kV Project and 15 kV Project, both plotted in the complex impedance plane (R, X).

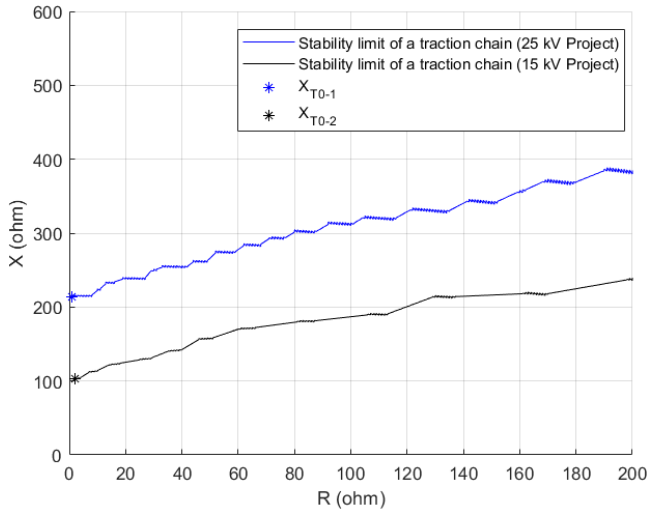

Fig. 18: Evolution of the stability limit as a function of the supply network (P_{dc} = 100 kW).

X_{T0} corresponds to the intersection of the stability limit curve and the vertical axis and can be considered as a distinctive parameter of a given traction chain.

X_{T0} value obtained for the 15 kV Project is lower than the value obtained for the 25 kV Project which is coherent with the network frequency ratio. Nevertheless, it should be noted that the ratio is not exactly three (frequencies ratio) because there are other factors which may influence the stability limit (the value of DC link capacitance (C_{bus}) and secondary winding leakage inductance (L_s)).

4 Influence of the number of independent traction chain on its stability limit

As explained in [3], [5], [6] a system composed of n identical traction chains is equivalent to a system with a single traction chain fed through the impedance $n \cdot Z$ (Fig. 19).

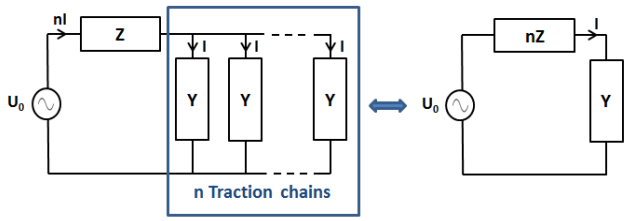

Fig. 19: Equivalence between the number of traction chains and the value of the network impedance.

As a result, the stability limit of a system composed of four identical traction chains of the 25 kV Project is determined by dividing the impedances allowing to bring a system with only one traction chain to its stability limit. This was verified by simulation by multiplying by four the current drawn by a traction chain (Fig. 20).

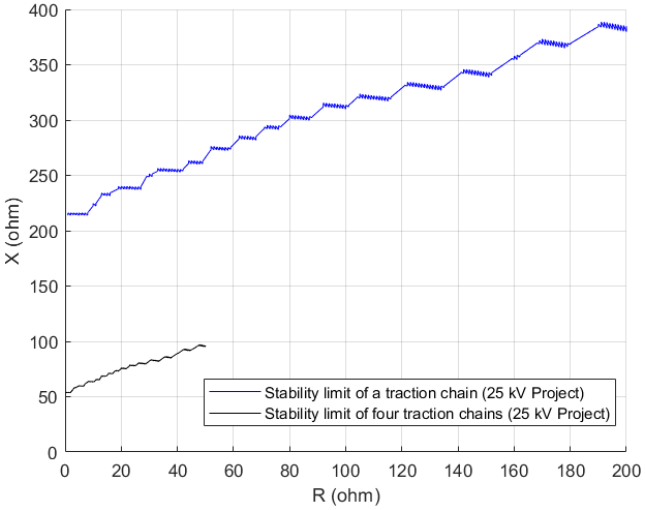

Fig. 20: Stability limit of a system with four traction chains supplied by a 25 kV / 50 Hz network.

5 Influence of the number of non-independent 4-Q rectifiers in a traction chain on its stability limit

In the previous section, two 4-Q rectifiers were functional. In this section, the traction chain is the same as shown in Fig. 3 but one 4-Q rectifier is inhibited. Figure 21 highlights the influence of the number of non-independent 4-Q rectifiers on the stability limit curves.

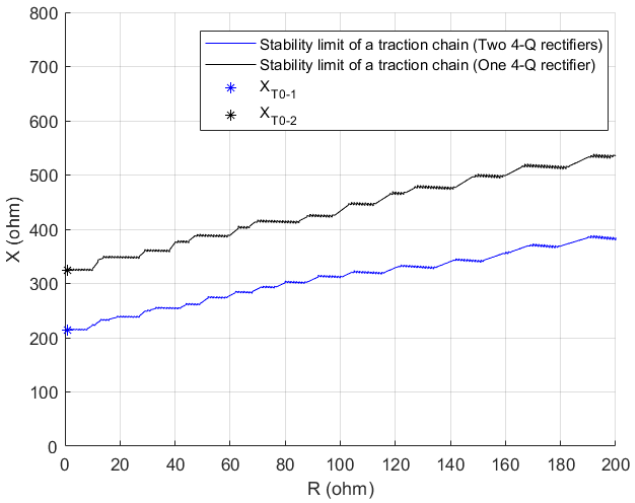

Fig. 21: Stability limit curve of a system with one 4-Q rectifier.

It can be seen that the stability limit of a traction chain with one 4-Q rectifier has increased.

According to section 4, the limit of stability depends on the number of traction chains and the installed power on a locomotive. Theoretically the number of MW.Ohms (X_{T0} × installed power) is expected to remain constant. In this example, since the installed power is divided by two the value of $X_{T0\text{-}1}$ should reach 400 Ω to keep the same MW.Ohms product. Nevertheless, this is not exactly true because the value of DC link capacitance (C_{bus}) was kept constant for the two cases.

6 Conclusion

The stability study of a traction system for different values of network impedance (R, L) was presented in this paper. This study is based on a simple graphical method based on the plot of the stability limit curve in the complex impedance plane (R, X). This method was applied to two different projects (15 kV Project and 25 kV Project). All the results obtained in the frequency domain were validated by simulations in the time domain.

It should be noted that the distinctive parameter X_{T0} obtained for the 15 kV Project is lower than the value obtained for the 25 kV Project. The ratio between these two impedance values does not correspond exactly to the ratio of the network frequencies. In fact, other parameters, such as the values of the DC link capacitance (C_{bus}) and the secondary winding leakage indutance (L_s), can influence the stability limit. Other studies are therefore necessary in order to better understand this difference.

7 References:

[1] D. Frugier, P. Ladoux: Voltage Disturbances on 25kV-50 Hz Railway Lines. Modelling Method and Analysis, SPEEDAM'10, IEEE International symposium on power electronics, electrical drives, automation and motion, PISA (Italie), June 2010.

[2] S. Danielsen: Electric Traction Power System Stability: Low Frequency interaction between advanced rail vehicles and a rotary frequency converter, PhD Thesis, Norwegian University of Science and Technology, Trondheim, Norway, April 2010.

[3] J. Suarez: Etude et modélisation des interactions électriques entre les engins et les installations fixes de traction électrique 25 kV/50 Hz, PhD Thesis, University of Toulouse, December 2014.

[4] E. Guillaume, H. Caron, P. Ladoux, N. Roux: Low frequency instability of electrical railways networks, WCRR'13 – World Congress on Railway Research, Sydney, Australia, November 2013.

[5] Y. Hachicha, D. Cypers, M. Takuefou, S. Belin, P. Ladoux and N. Roux: Use of a HIL railway traction simulator for low frequency network stability studies, IEEE International Conference on Electrical Systems for Aircraft, Railway, Ship Propulsion and Road Vehicles & International Transportation Electrification Conference (ESARS-ITEC), Nottingham, November 2018.

[6] Y. Hachicha, D. Cypers, M. Meli, S. Belin, P. Ladoux and N. Roux: 50 Hz Railway Power System Low-frequency Stability Limit determination as a function of D-Q Train Admittance and Network Impedance, Elektrische Bahnen Journal, 2020.